

# Survey Techniques to Examine Morphological Evolution of Coastal Regions

by

Seth N Ammons

Submitted to the Department of Mechanical Engineering, MIT in partial fulfillment of the requirements for the degree of

MASTER OF SCIENCE IN MECHANICAL ENGINEERING

at the

MASSACHUSETTS INSTITUTE OF TECHNOLOGY

September 2024

© 2024 S. N. Ammons. All rights reserved

The author hereby grants to MIT a nonexclusive, worldwide, irrevocable, royalty-free license to exercise any and all rights under copyright, including to reproduce, preserve, distribute and publicly display copies of the thesis, or release the thesis under an open-access license.

Authored by: Seth N. Ammons  
Department of Mechanical Engineering, MIT  
Applied Ocean Science & Engineering, WHOI  
August 01, 2024

Certified By: Britt Raubenheimer  
Senior Scientist, Applied Ocean Physics & Engineering, WHOI, Thesis Supervisor

Certified by: Steve Elgar  
Senior Scientist, Applied Ocean Physics & Engineering, WHOI, Thesis Supervisor

Accepted by: Alexandra H. Techet  
Professor of Ocean and Mechanical Engineering, MIT  
Chair, Joint Committee for Applied Ocean Science & Engineering

Accepted by: Nicolas Hadjiconstantinou  
Professor of Mechanical Engineering, MIT  
Chair, Department Committee on Graduate Students



# Survey Techniques to Examine Morphological Evolution of Coastal Regions

by

Seth N Ammons

Submitted to the Department of Mechanical Engineering on August 01, 2024 in partial fulfillment for the degree of

MASTER OF SCIENCE IN MECHANICAL ENGINEERING

## **Abstract**

Beaches are dynamic, changing with tides, winds, and waves. Here, a beach was mapped daily for 3 weeks from the dune to the low-tide water line on the Outer Banks of North Carolina at the US Army Corps of Engineers Field Research Facility in Duck. The 22,500 m<sup>2</sup> area of interest was surveyed daily by a walker carrying a GPS-equipped backpack and occasionally with a lidar equipped drone. Surveys of the northern region of interest also were collected with a stationary terrestrial lidar mounted on the dune. The observed morphological events include the destruction and formation of a cusp field during which there was 1.4 m of erosion and accretion associated with bays and horns, and the formation over 7 days of a ~1-m high ridge and runnel system. The GPS-equipped backpack apparatus was used as ground truth for estimates made with the lidar systems. Along both cross- and alongshore transects the lidar elevations were within approximately 0.05 m of those estimated by the backpack surveys, with RMS errors less than 0.11 m.

Thesis Supervisor: Britt Raubenheimer  
Title: Senior Scientist, WHOI

Thesis Supervisor: Steve Elgar  
Title: Senior Scientist, WHOI





## **Acknowledgments**

Thank you to the several groups of institutions and mentors that have provided me the opportunity to pursue higher education at the Massachusetts Institute of Technology – Woods Hole Oceanographic Institution. Broadly, thank you to the United States Navy and the Submarine force for continuing to provide a realistic path and funding for junior officers to pursue higher education while serving that compliments the trajectory of our careers.

I am incredibly thankful for the leadership and mentorship that I had been blessed with throughout my naval career, and it was no different at my first duty station. I appreciate every person that I had the honor of serving alongside at-sea in my first tour and inspiring me to continue my career in the submarine force and pursue higher education through the MIT-WHOI Joint Program. Without much direction, or ambition for a career in the military upon showing up to my first command, my Captain Will Wiley, Engineer Kristin Shaw, Chief of the Boat Tony Amato, and Auxiliary Division Chief Jared Fouke have my sincerest gratitude for their mentorship and being models of the concept of relentlessly pursuing excellence in every aspect of our lives. In the pursuit of a standard of excellence, they taught me to continuously challenge myself leading to the decision to apply to the MIT-WHOI Joint Program.

Coming into the academic world, having not been in a formal classroom setting in a significant amount of time, thank you to my advisors Steve Elgar and Britt Raubenheimer. I greatly appreciate the patience that they have continuously showed me throughout the two years balancing class work and research. In the course of research, it was great to be able to experience the process of conducting field work from start to finish and I would be remiss if I didn't thank the both of them for accompanying me on the daily 3.5-mile walks on the beach conducting surveys, sharing their wisdom, and stories that I won't forget. Last but not least, thank you for the mentorship throughout the last two years. I'm not sure that I could have effectively navigated the rigors of the academic world without their guidance and encouragement.

Thanks to the Field Research Facility field crew in Duck, North Carolina, and Ciara Dooley, Charles Murman, Austin Faddish, Alex Muscalus, and MP Delisle for help with fieldwork. A

special thank you to Levi Gorrell for the endless hours of troubleshooting code to efficiently process data. For those that I have failed to mention but have impacted my career pursuits, thank you for your support. Funding was provided by the Office of Naval Research, the National Science Foundation, and a Vannevar Bush Faculty Fellowship.



# Table Of Contents

<b>Title Page</b> .....	<b>1</b>
<b>Abstract</b> .....	<b>3</b>
<b>Acknowledgments</b> .....	<b>5</b>
<b>Chapter 1 Introduction</b> .....	<b>11</b>
1.2 Cusp Field Dynamics .....	13
1.3 Ridge and Runnel Dynamics .....	14
<b>Chapter 2 Observations of Beach Evolution</b> .....	<b>15</b>
2.1 Field Measurements .....	15
2.2 Cusp Field Observation.....	20
2.2.1 Cusp Destruction.....	20
2.2.2 Cusp Formation.....	22
2.3 Ridge and Runnel Formation .....	24
<b>Chapter 3 Survey Technique Comparison</b> .....	<b>27</b>
3.1 Backpack Surveys.....	27
3.2 DJI Matrice 300 / Zenmuse L1 Lidar Payload.....	29
3.3 Stationary Terrestrial Lidar .....	31
3.4 Survey Technique Comparison .....	32
<b>Chapter 4 Conclusions</b> .....	<b>36</b>
<b>References</b> .....	<b>38</b>

# List of Figures

Figure 2.1: (a) Aerial image of the study area spanning 450 m alongshore by 50 m cross-shore north of the pier at the Field Research Facility, Duck, NC, and (b) 3D and (c) 2D views of sand levels (color contours relative to NAVD88, key at top) measured with a backpack survey on 10/09 2023. .... 16

Figure 2.2: Daily backpack surveys between the dune toe and the ocean were conducted requiring walking ~5-6 km (~100-120 km over the 3-week study). The backpack contains a strap and harness system housing a Trimble R7 GPS receiver with an attached Trimble Zephyr Geodetic antenna..... 17

Figure 2.3: (a) Significant wave height, (b) wave direction, and (c) mean wave period measured in 17-m water depth (NDBC buoy 44056) versus date in 2023. Periods of interest highlighted based on the event observed include cusp destruction (red), cusp formation (green), and ridge and runnel system formation (orange). The horizontal black line in panel (b) indicates the angle of normal incidence ( $72^\circ$  true north)..... 19

Figure 2.4: Sand levels (color contours relative to NAVD88, key at top) measured with a backpack survey on (a) 09/12 and (b) 09/16 2023 as a function of the cross- and alongshore coordinates. (c) Total change in sand levels between 09/12 and 09/16 along the transect for  $x=85$  m (horizontal blue line in a and b) versus alongshore coordinate during the cusp destruction event..... 20

Figure 2.5: (a) Elevation along cross-shore transect  $x=85$  m versus alongshore coordinate between 09/12 and 09/16 (legend in the upper right), and daily elevation change versus alongshore coordinate from (b) 09/12 to 09/14, (c) 09/14 to 09/15, and (d) 09/15 to 09/16..... 21

Figure 2.6: (a) Sand levels (color contours relative to NAVD88, key at top) measured with a backpack survey on 09/30 and (b) 10/04 2023 as a function of the cross-shore and alongshore coordinates. (c) Total change in sand levels between 09/30 and 10/04 along the transect for  $x=85$  m (horizontal blue line in a and b) versus alongshore coordinate during a cusp formation event. .... 22

Figure 2.7: (a) Elevation along cross-shore transect ( $X=85$  m) versus alongshore coordinate between 09/28 and 10/04 (legend in the upper right), and daily elevation change versus alongshore coordinate from (b) 09/30 to 10/01, (c) 10/01 to 10/02, (d) 10/02 to 10/03, and (e) 10/03 to 10/04. Arrows in (b) indicate cusp migration to the south. .... 23

Figure 2.8: (a) Sand levels (color contours relative to NAVD88, key at top) measured with a backpack survey on 10/03 and (b) 10/10 2023 as a function of the cross-shore and alongshore coordinates. (c) Total change in sand levels along the transect for  $y=600$  (vertical lines) as a function of cross-shore coordinate during a ridge and runnel formation event..... 25

Figure 2.9: (a) Elevation along an alongshore transect ( $y=600$  m) versus cross-shore coordinate between 10/03 and 10/10 (legend in the upper right), and daily elevation change versus cross-shore coordinate from (b) 10/03 to 10/05, (c) 10/05 to 10/07, and (d) 10/07 to 10/10..... 26

Figure 3.1: Backpack apparatus with Trimble GPS receiver in yellow box on the left and the base station tripod and accompanying Trimble GPS antenna on the right. .... 28

Figure 3.2: DJI Matrice M300 with Zenmuse L1 payload attachment..... 30

Figure 3.3: Elevation of the beach versus alongshore coordinate for backpack (black), drone lidar (red), and stationary dune lidar (blue) surveys conducted on 10/02. Stationary dune lidar data (blue) adjusted 0.05 m to account for offset in raw data. .... 33

Figure 3.4: Elevation of the beach versus cross-shore coordinate for backpack (black), drone lidar (red), and stationary dune lidar (blue) surveys conducted on (a) 10/02 2023 and (b) 10/05 2023 (in b the dune lidar did not extend as far south as  $y=600$  m)..... 34

# Chapter 1 Introduction

Understanding the dynamics that drive topographical evolution of coastal regions directly impacts the ability to sustain and protect the socioeconomic interests that drive large portions of the world population to the coastline (Vousdoukas et. al, 2020). The ability to model the coastline at high spatial and temporal resolution provides insight into the sediment transport feedback processes that result from tides and waves, improving the ability to forecast projected shoreline adjustments as a result of infrequent meteorological events such as storms that result in high wave energy characteristics with large shoreline run-up (Mentaschi et. al, 2018). The most effective means of data collection to contribute to the understanding of the dynamic shaping of the coastline is dependent on the scale of the area of interest. Aerial imagery-resolved-structure from motion, aerial and stationary laser detection and ranging systems, vehicle sonar systems, or global positioning system (GPS) systems readily are deployed on small spatial scales with varied temporal resolution. For large spatial scale analysis, satellite imagery and lidar have become the primary means of data collection with improvement and accessibility of data processing software (Luijendijk et. al, 2018). The goals here of high spatial (order 1 m) and temporal (daily) resolution surveys over a 450 m stretch of beach from the dune to the low-tide water line required the use of accurate land-based survey techniques that were controlled by the surveyor who could increase the density of data near areas of interest.

The area of interest covers 22,500 m<sup>2</sup> along the Outer Banks, North Carolina on the Atlantic Coast at the United States Army Corps Field Research Facility (FRF) in Duck. This beach is characteristically sandy with a large dune system that protects the inland coastal socioeconomic interests of the region. While long term erosion of the barrier islands is of interest, the foundation for modeling the projected long-term effects of hydrodynamic and meteorological processes on shaping the topography of the coastline is dependent on the ability to observe and analyze the adaptation of the coastline to tidal cycles, the incident wave characteristics, and storm conditions. The nearshore topography and bathymetry are surveyed monthly along cross-shore transects spaced 46 m in the alongshore by the FRF staff using a GPS and sonar equipped lighter amphibious resupply cargo vehicle (LARC) and coastal research amphibious buggy (CRAB,

Birkemeier & Mason, 1984) and a part of the beach is surveyed hourly with a stationary lidar system.

While providing opportunity for efficiently mapping the transition from topography to bathymetry, the CRAB and LARC are slow (3.2 km/hr and 7 km/hr respectively) and require significant planning for qualified personnel and favorable sea state conditions with low significant wave height (<1.5 and <1 m, respectively) (Birkemeier & Mason, 1984) (Forte et. al, 2017). Moreover, their relatively large foot print caused by the several meters of separation of the tires reduces the spatial resolution of horizontal positions and elevations considerably.

A potentially higher-spatial resolution alternative GPS topographical surveying method is a backpack apparatus that is worn by an individual capable of covering the immediate transition from topography to bathymetry and provides flexibility in the execution of the survey patterns and emphasis around small topographic features. As an alternate survey method for topographic surveying, backpack surveys provide a great advantage in resolution and the method is independent of hydrodynamic conditions based on the bathymetry surveying being restricted by the depth to which the surveyor can wade into the water without submerging the GPS equipment.

Alternative survey techniques include lidar systems mounted on a tower on the beach or on a drone flying over the beach (O'Dea et. al, 2019). At the FRF, a dune-mounted terrestrial lidar is continuously operated (Chapter 3), but is restricted to a field of view of about 200 m alongshore, and can be shadowed by features in the beach (e.g., beach cusp horns). In contrast, lidar equipped drones provide the flexibility to expand the area of interest to as large as flight logistics allow, and for flight paths specific to the research priorities to be designed (Chapter 3). However, based on the drone technology of choice, lidar equipped drones are restricted by battery life and meteorological conditions, limiting the ability to perform surveys in all conditions. Here, drone- and tower-mounted lidar surveys of the beach are compared with those made by a walking with a GPS-equipped backpack.



## 1.1 Objectives

The complexity of the coastal environment makes consistent, long term, data collection difficult (O’Dea et. al, 2019). Remote sensing provides the ability, and an opportunity, to remove the necessity of installing sensors and hardware directly into the research field, as well as removing the need for personnel to navigate the unpredictability of the surfzone to install and remove such hardware. One of the purposes of this study was to examine the applicability of different survey techniques to provide daily topographical observations of beach morphological evolution in response to a range of incident wave conditions and meteorological events.

Over a 3-week period the beach was surveyed daily by people walking with a GPS-equipped backpack, occasionally by a drone carrying a survey lidar, and hourly by a lidar mounted on a dune at one end of the study site. The surveys from the different techniques are similar to each other, with vertical differences of a few cm. The observations include the destruction and formation of beach cusps, and the growth of a ridge and runnel system.

The objectives of this study are:

1. To conduct high resolution surveys of the daily morphological evolution at the sea-land interface as a result of hydrodynamic forcing and feedback processes.
2. Analyze the applicability of remote sensing using a drone with lidar technology as an alternative to current GPS survey methods and practices.

## 1.2 Cusp Field Dynamics

Beach cusps are characterized as a topographical feature that includes elevated horns separated by a depressed outflow channel that often repeats in a rhythmic pattern for multiple kilometers in the alongshore (Coco & Murray 2007, O’Dea et al. 2024). Several theories and hypotheses have been proposed to explain cusp formation, including standing edge waves and hydrodynamic forced sediment transport (self-organization) (Coco & Murray 2007).

Standing edge waves were an early explanation to the formation of the rhythmic patterns in the dynamic near shore that is constantly stressed by hydrodynamic interaction (Guza & Davis

1974). Edge waves are alongshore-propagating gravity waves that become trapped due to refraction, with the highest amplitude at the shoreline. When edge waves propagate both up and down the beach, standing patterns develop with “nodes” with near-zero amplitude separated by “anti-nodes” at which amplitudes are maximum. The standing pattern is reflected in the topography with horns at nodes and bays at the anti-nodes. The standing wave theory for beach cusps suggests the cusps and edge waves grow together with cusp spacing that depends on beach slope and edge-wave characteristics (Guza & Davis 1974).

In contrast to the standing-wave theory, self-organization is a feedback model between the hydrodynamic forcing in the swash zone and coastal morphology (Werner & Fink 1993, Coco & Murray 2007). The forcing mechanism for the formation of a cusp system can be attributed to natural reinforcement of hydrodynamic conditions. Inherent imperfections in the nearshore topography (e.g., small pits or lumps owing to biological activity, shell deposits, or other processes) result in flow accelerations in depressions and decelerations over bumps resulting in positive feedbacks with continued erosion and accretion of areas with low and high sand levels, respectively. As the higher elevation areas continue to accrete, and the depressed channels continue to erode the coastline will reach a steady state stabilizing the horn and bay system (Werner & Fink 1993).

### **1.3 Ridge and Runnel Dynamics**

Beach recovery is important in countering the offshore sediment transport and erosion that occurs as a result of high energy waves during storms. Onshore sand bar migration during moderate waves contributes to large influxes of sediment to the shoreline that protect the inner coastal regions from high water levels and wave energy (Figlus et al. 2012, Biaisque et al. 2020). Intertidal bars transported onshore as a ridge and runnel system are characterized as an emergent berm that stands between the ocean and a smaller alongshore-oriented secondary body of water behind the ridge that directs water to flow via a channel back offshore (Figlus et al. 2012, Biaisque et al. 2020). Previous studies and observations vary in defining the attributes of these systems, but are consistent in the hydrodynamic conditions that are the primary mechanisms in the morphological feedback that is required for reinforcement and sustainment of a ridge and runnel (Biaisque et al. 2020).

# Chapter 2 Observations of Beach Evolution

## 2.1 Field Measurements

Topographic surveys were collected from Sep 12 until Oct 10, 2023 over a 450-m alongshore by 50-m cross-shore stretch of the Atlantic Ocean beach north of the U.S. Army Corps of Engineers Field Research Facility (FRF) pier in Duck, North Carolina (Fig 2.1a). The site is on the northern Outer Banks, a barrier island system that stretches from the Virginia-North Carolina border to Oregon Inlet. The research facility is on a one-kilometer-wide stretch of land with the Atlantic Ocean to the east and the Currituck sound to the west fed by the Albemarle-Pamlico sound system with an opening at Oregon Inlet, about 30 miles south of the study site (Brodie et al. 2019). The wave-driven erosion of the dune systems throughout the Outer Banks has been offset partially by extensive dune nourishment projects in the region for inland protection (Cohn et al. 2021). To assess the natural evolution of beach and dune morphology, the beach at the FRF site has not been nourished since the initial creation of the dunes. The dunes at the study site range from 5-8 meters high, and are not overtopped, even during the largest storms (Cohn et al. 2021). Intertidal sediment is roughly uniform with median grain size about 0.3 mm (Cohn et al. 2021, 2022).

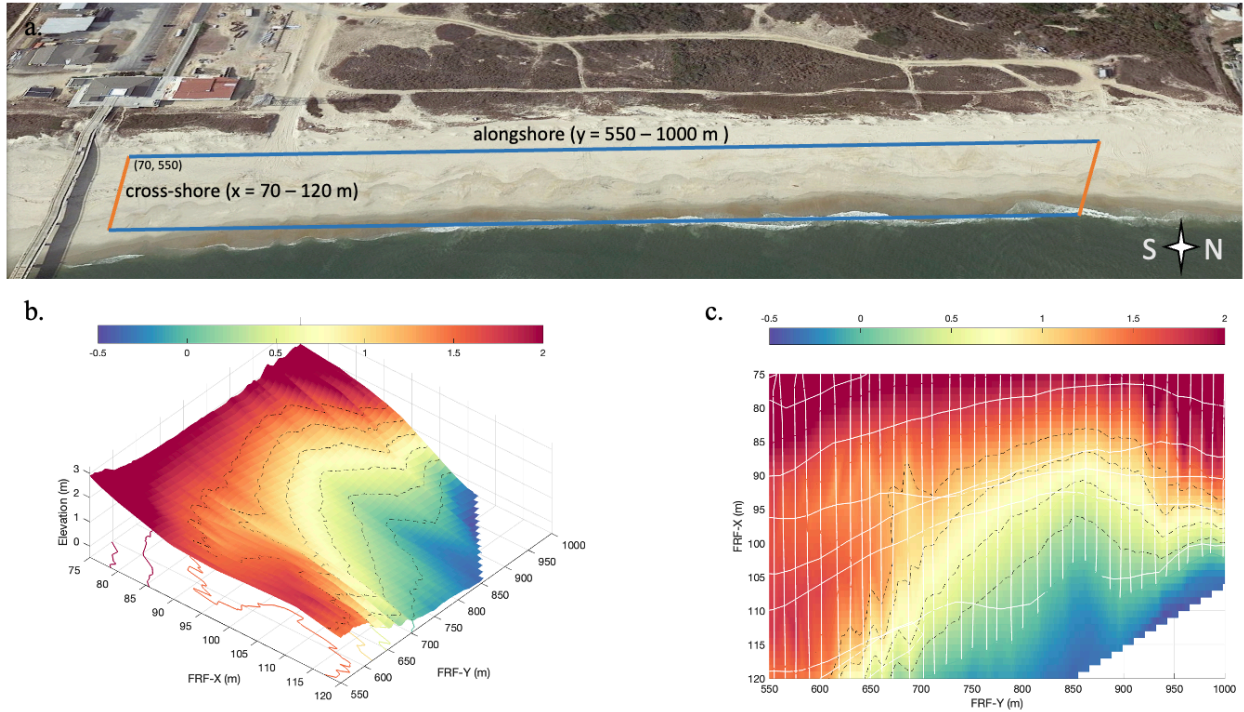


Figure 2.1: (a) Aerial image of the study area spanning 450 m alongshore by 50 m cross-shore north of the pier at the Field Research Facility, Duck, NC, and (b) 3D and (c) 2D views of sand levels (color contours relative to NAVD88, key at top) measured with a backpack survey on 10/09 2023.

The area of interest for this study is north of the FRF pier extending approximately 50 m in the cross-shore from the toe of the dunes to as deep in the water as a person carrying a backpack with survey gear could wade safely at low tide. The GPS-based survey data are obtained in latitude-longitude horizontal coordinates that are converted into a local grid space using the FRF coordinate system. Vertical elevations are referenced to the North American Vertical Datum 1988 (NAVD88) (Fig 2.1 a,b) (Brodie et al. 2019). For consistency in data processing across the three survey techniques employed throughout this study, the local FRF coordinates were converted to 1- by 1-m grids starting at the base of the pier and the dune toe at  $x = 70$  and  $y = 550$  m (Fig 2.1a).

Daily, within an hour of the daylight low tide, sand levels were surveyed using a GPS system sampled at 10 Hz contained in a backpack with surveying apparatus (Fig 2.2). A second GPS receiver was housed in a weatherproof case beneath the GPS antenna of a base station that was

mounted on a tripod over a benchmark on the northeast corner of the FRF pier deck to obtain data for post-processing.



*Figure 2.2: Daily backpack surveys between the dune toe and the ocean were conducted requiring walking ~5-6 km (~100-120 km over the 3-week study). The backpack contains a strap and harness system housing a Trimble R7 GPS receiver with an attached Trimble Zephyr Geodetic antenna.*

Daily, within an hour of the daylight low tide, a surveyor wearing the backpack system walked cross-shore transects covering the dry beach to about knee-deep water, followed by alongshore transects between the dune toe and lower intertidal (Fig 2.1 b,c). Transects were separated by approximately 10 m in both the alongshore and cross-shore. Additional survey transects were conducted to increase the spatial resolution near areas with noticeable (steeper than the typical beach slope) topographic features. The additional transects were performed at 2-m spacing in the

alongshore and cross-shore covering the entire area of interest. More than 5-6 km were traversed each day. Although coverage is attainable by means of daily backpack surveying, the time and personnel required to accomplish these surveys is not a sustainable practice over long periods, supporting the need for alternate surveying techniques. To provide consistent surveying over the duration of the study, and to minimize the personnel impact of this technique, two individuals alternated the responsibility of daily backpack surveys. The elevation of the GPS antenna above the ground was measured following each survey to account for slight changes in the positioning of the backpack apparatus and small differences ( $\sim 0.02$  m) in height between the two surveyors to minimize error.

During the study, the semi-diurnal tide ranged over  $\sim 1.3$  m, significant wave heights (Fig. 2.3a), wave directions (Fig. 2.3b), and mean wave periods (Fig. 2.3c) measured with a National Oceanographic and Atmospheric Administration (NOAA) wave-rider buoy in 17-meter water depth ranged from near 0 to almost 6 m, from about 10 to 130 degrees relative to north, and from 4 to 12 seconds, respectively.

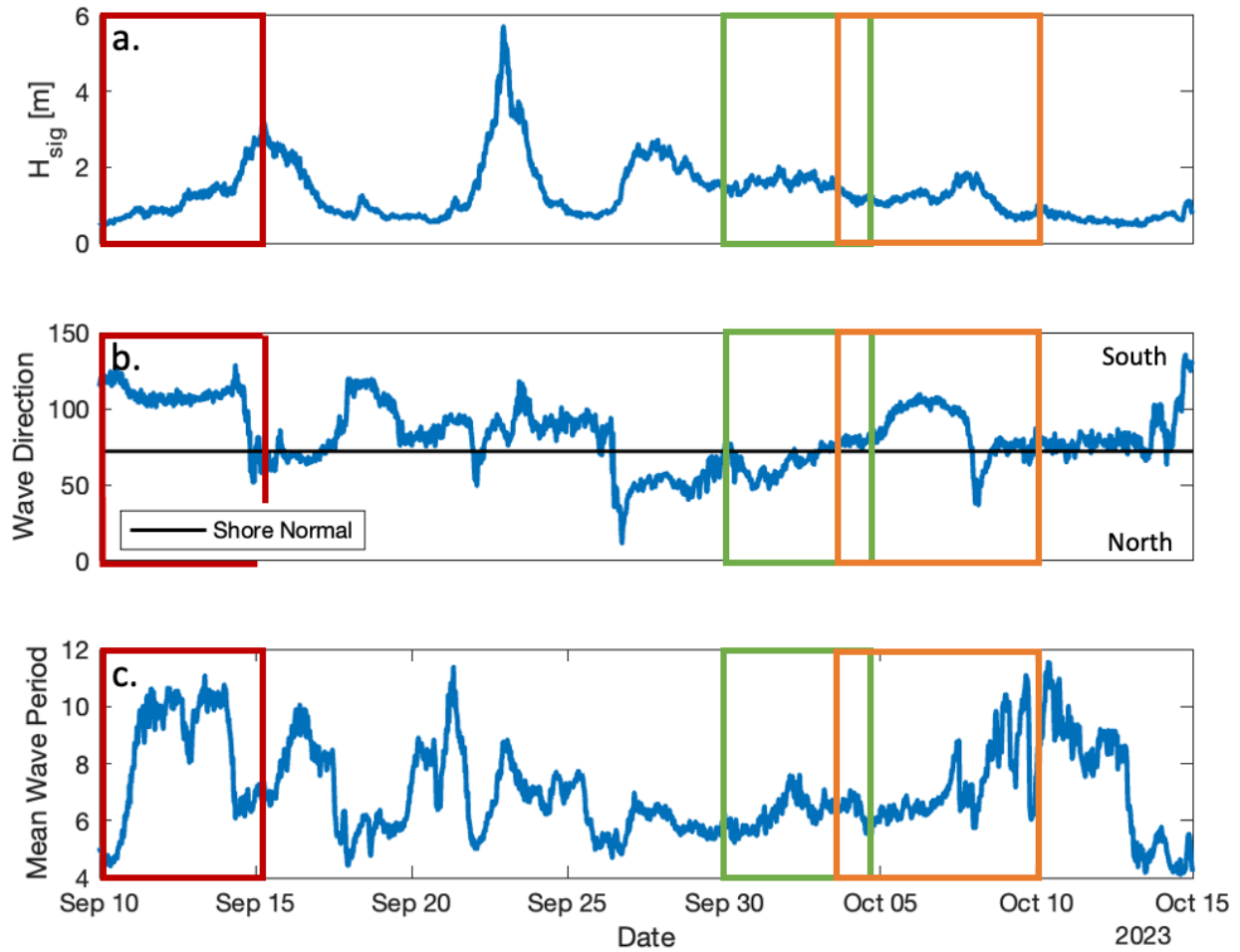


Figure 2.3: (a) Significant wave height, (b) wave direction, and (c) mean wave period measured in 17-m water depth (NDBC buoy 44056) versus date in 2023. Periods of interest highlighted based on the event observed include cusp destruction (red), cusp formation (green), and ridge and runnel system formation (orange). The horizontal black line in panel (b) indicates the angle of normal incidence ( $72^\circ$  true north).

Beach cusps were present at the northern end of the survey area at the start of the study period and were eroded as waves from the north increased in height (Fig 2.3, red boxes). Beach cusps re-formed in the same area later during a period of small, near normally incident waves (Fig 2.3, green boxes). Near the end of the study, a ridge and runnel system moved onshore in the southern portion of the study area (Fig 2.3, orange boxes).



## 2.2 Cusp Field Observation

Consistent with this study, collecting beach cusp data sets that include the environmental forcing functions of cusp formation at high spatial and temporal resolution is complicated and expensive, leading to studies that focus on a small number of cusp generation and destruction events occurring over a short period of time (O’Dea et al. 2024). Characteristic of the nearshore, low-tide region covered, the formation and destruction event of cusp systems can develop rapidly over only a few days and potentially over a single tidal cycle owing to the dynamic interaction of the swash flows with the shoreline sediments. During the three-week period, one cusp destruction and one cusp formation event were observed with the high-resolution surveys.

### 2.2.1 Cusp Destruction

Three prominent elevated horns extending offshore accompanied by two depressed outflow channels, characteristic of beach cusps, spanned rhythmically alongshore from  $y = 820$  to  $900$  m at the commencement of data collection on September 12 (Fig 2.4a) (Coco & Murray 2007, O’Dea et al. 2024). The horns measured  $10$  m in width with  $20$ -m-wide outflow channels. Initial significant wave height and wave period were  $0.5$  m and  $4$  s, respectively, with incident waves approaching the coastline from the south (Fig 2.3).

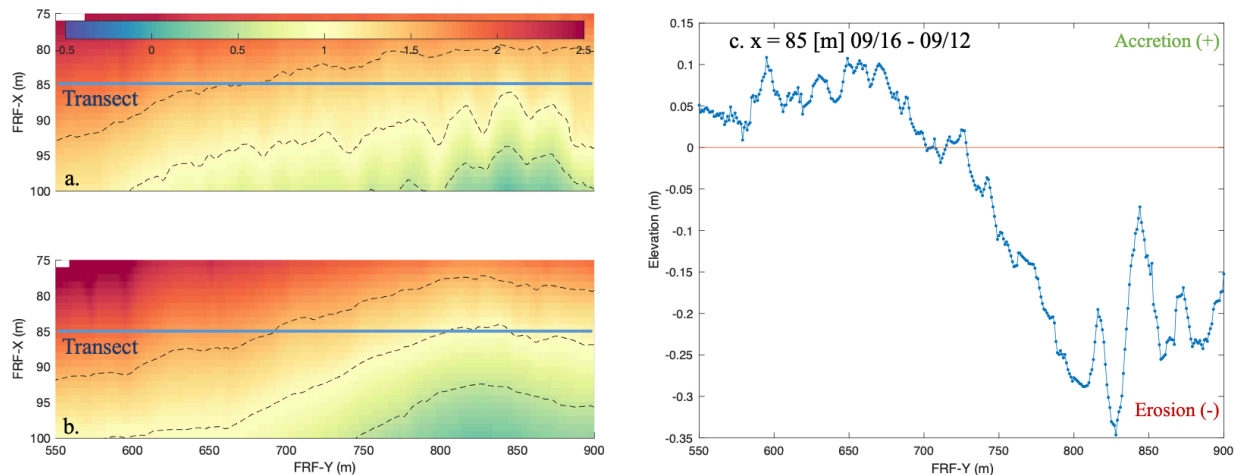


Figure 2.4: Sand levels (color contours relative to NAVD88, key at top) measured with a backpack survey on (a) 09/12 and (b) 09/16 2023 as a function of the cross- and alongshore coordinates. (c) Total change in sand levels between 09/12 and 09/16 along the transect for  $x=85$



$m$  (horizontal blue line in a and b) versus alongshore coordinate during the cusp destruction event.

As winds shifted, waves from the south increased in height (red boxes in Fig. 2.3), and the cusps slowly were eroded (Fig. 2.5).

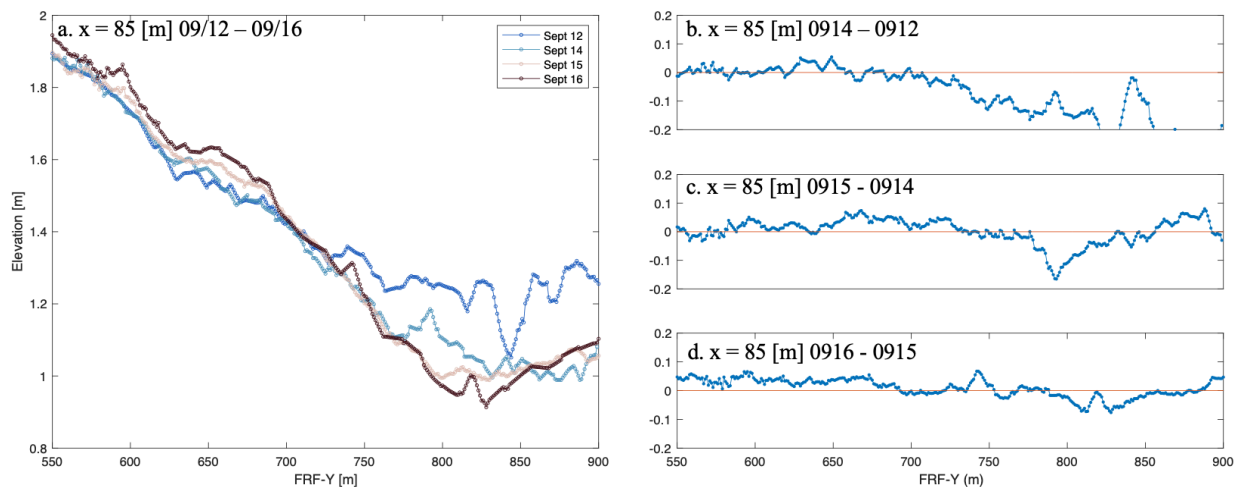


Figure 2.5: (a) Elevation along cross-shore transect  $x = 85$  m versus alongshore coordinate between 09/12 and 09/16 (legend in the upper right), and daily elevation change versus alongshore coordinate from (b) 09/12 to 09/14, (c) 09/14 to 09/15, and (d) 09/15 to 09/16.

The sustainment of beach cusp systems is reliant on the stability of the hydrodynamic forces interacting with the shoreline (O’Dea et al. 2021). At steady state, the flow velocity interacting with the beach cusp system is no longer contributing to the accretion and erosion of the horn and bay features ending the formation process (Werner & Fink 1993, Coco & Murray 2007). As the significant wave height increased from 0.5 to 2 m (Fig 2.3a) and the wave direction shifted from the south to near normally incident (Fig 2.3b), the beach cusps eroded, consistent with smoothing of the beach cusps by negative hydrodynamic feedbacks (Coco et al. 2003).

Initially, the difference in elevation between the horns and bays was  $\sim 0.5$  m. By the survey on 09/14, the cusps had eroded to a smooth surface (along a contour, Fig 2.4b), with both the horns eroding more than the bays (Fig 2.4c). Following the destruction of the beach cusp system, the beach profile stabilized, with minimal topographic features by 09/16.

Over the 48 hours from the initial survey on 09/12 to the flattening of the cusp field on 09/14 (Fig 2.5a) approximately  $35 \text{ m}^2/\text{m}$  of sediment was eroded along the northern section ( $y > 700 \text{ m}$ , Fig. 2.4) of the alongshore transect at cross-shore location  $x=85 \text{ m}$ , and possibly led to the accretion to the south ( $y < 700 \text{ m}$ , Fig. 2.4).

### 2.2.2 Cusp Formation

The beach elevation remained relatively stable from mid- to late-September (not shown). Toward the end of September, the topography of the survey area and predicted hydrodynamic conditions indicated favorable prerequisites for the formation of a cusp field in the same location that cusp destruction was observed earlier in the study (Coco & Murray 2007). Before the cusps formed, the alongshore transect at  $x = 85 \text{ m}$  was smooth in the alongshore, and the topography in the cross-shore between  $y = 900$  and  $1000 \text{ m}$  had a  $0.067$  slope from  $2\text{-m}$  elevation at the toe of the dune to  $0 \text{ m}$  at the waterline (Fig 2.6a).

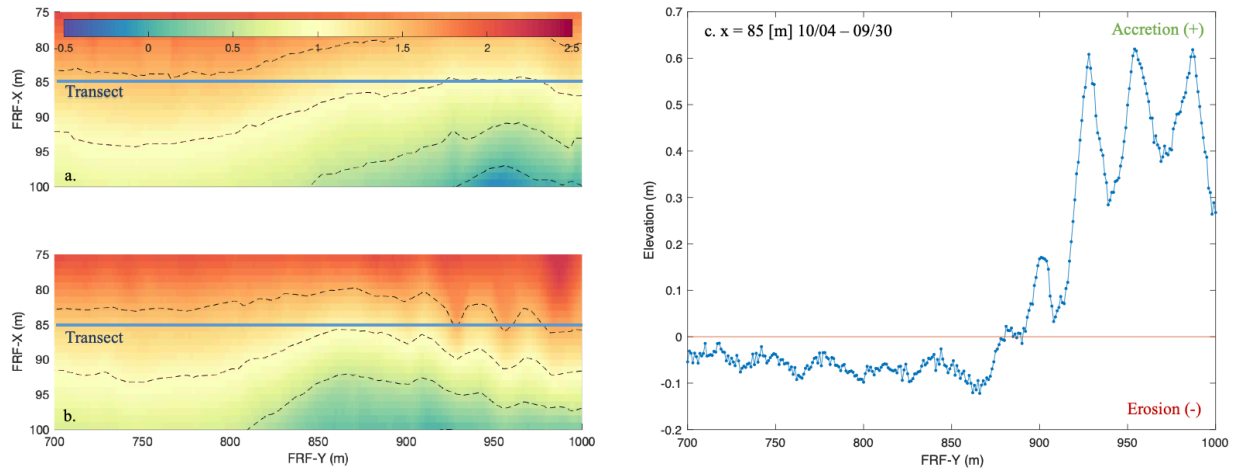


Figure 2.6: (a) Sand levels (color contours relative to NAVD88, key at top) measured with a backpack survey on 09/30 and (b) 10/04 2023 as a function of the cross-shore and alongshore coordinates. (c) Total change in sand levels between 09/30 and 10/04 along the transect for  $x=85 \text{ m}$  (horizontal blue line in a and b) versus alongshore coordinate during a cusp formation event.

The accretion in the days leading up to the formation of the cusp field supports previous

observations of onshore sediment transport as a result of low energy hydrodynamic conditions in beaches with small tidal ranges (Kroos & Messelink 2002). The elevation at the  $x = 85$  m alongshore transect increased from 0.5 to 1.0 m between 09/28 and 09/30 for  $y > 900$  m, with no change in elevation in the southern portion ( $y < 800$  m) of the survey area (Fig. 2.7a). The introduction of sediment transported onshore based on the low energy wave conditions is reinforced with continued accretion throughout the cusp formation event (Fig 2.7a).

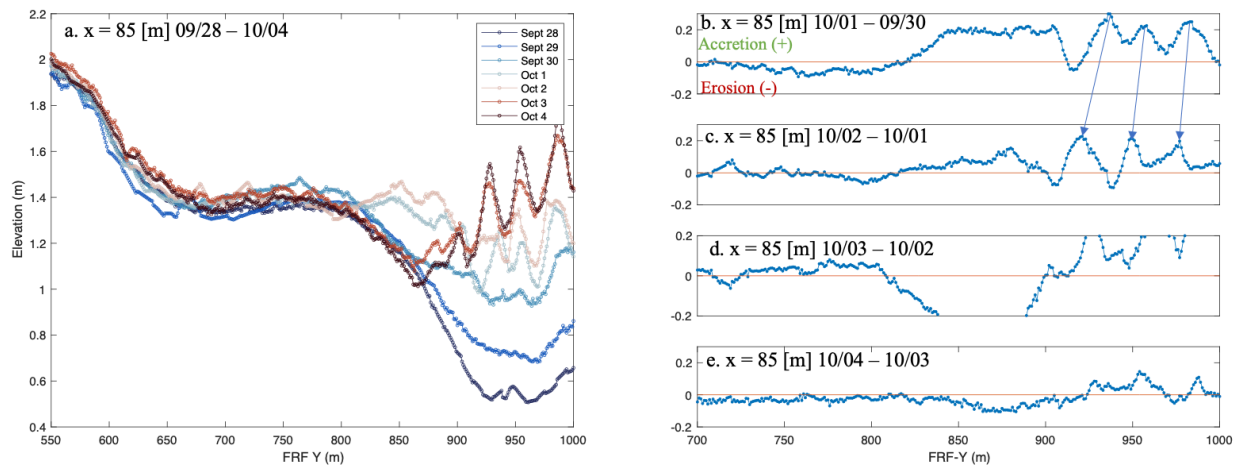


Figure 2.7: (a) Elevation along cross-shore transect ( $X= 85$  m) versus alongshore coordinate between 09/28 and 10/04 (legend in the upper right), and daily elevation change versus alongshore coordinate from (b) 09/30 to 10/01, (c) 10/01 to 10/02, (d) 10/02 to 10/03, and (e) 10/03 to 10/04. Arrows in (b) indicate cusp migration to the south.

The significant wave height remained low and constant (Fig 2.3a), the mean wave period began to increase (Fig 2.3c), and incident wave direction moved from the north to near normally incident (Fig 2.3b), possibly creating an instability in the shoreline primed for cusp formation (Kroon & Messelink 2002). Low energy waves with constant incident wave direction are favorable initial conditions for the formation and reinforcement of beach cusp systems (O’Dea et al. 2024), consistent with the observations here. The cusp formation occurred over one tidal cycle from 09/30 to 10/01 (Fig. 2.7), and over multiple days evolved into a cusp system between  $y = 900$  and 1000 m (Figs. 2.6 & 2.7). Accretion began at the north end of the survey area with 1-m high (green box in Fig. 2.3a), 5-s period (Fig. 2.3c) waves (Fig 2.3a) from the north (Fig 2.3b).

Between 09/30 and 10/01, the primary forcing mechanism for the formation of cusps, based on other constant wave characteristics (Fig 2.3), is a shift in incident wave direction from directly onshore to 50 degrees relative to north (Fig 2.3b), which may have introduced the instability required to promote cusp formation. Three prominent horns form on 10/01 with 0.2 m accretion (Fig 2.7b). The bays that formed were not a result of an erosive process from the steady state beach profile, but were formed primarily as minima in accretion between the rapidly accreting horns (Fig 2.7b). Following the initial creation of the cusp system, the wave energy remained low, but the incident wave direction began to shift from 50 degrees relative to north to coming slightly from the south (80 degrees relative to north) (Fig 2.3b). By 10/02, the horns moved south 15 m (arrows in Fig. 2.7b) and accreted an additional 0.2 m while the bays were reinforced by minor erosion (Fig 2.7b). As the incident wave direction shifted from onshore to from the south, the entire cusp system was reinforced with continued accretion of  $\sim 0.1$  m per day, raising the entire system by another 0.2 m by 10/04.

The magnitude of change in wave characteristics during this event was small, with the exception of the changing wave direction. Three prominent cusps formed, migrated 25 m to the south, and were reinforced by continued accretion resulting in  $\sim 1$  m increase in sand-level elevation at the cups horns (Fig 2.7a). The overall accretion during the cusp formation accounts for  $60 \text{ m}^2/\text{m}$  along the alongshore transect at  $x = 85 \text{ m}$  (Fig 2.6c).

### **2.3 Ridge and Runnel Formation**

The formation of a ridge and runnel system occurred over a week between 10/03 and 10/10 (Figs. 2.8 & 2.9) between  $y = 550$  and  $700 \text{ m}$  at the southern region of the survey area (Fig 2.8b), resembling the surfzone bathymetry containing one or two shallow sandbars at approximately  $y = 600$  to  $800 \text{ m}$  (not shown) that are separated alongshore by a deep channel. Throughout the formation of the ridge and runnel system, significant wave height was roughly constant at about  $1 \text{ m}$  (Fig 2.3a), the mean wave period increased from  $6$  to  $10 \text{ s}$  (Fig 2.3c), and the incident wave direction increased its angle of approach from the south during the accretion of the ridge before rapidly shifting to the north reinforcing the system, then back to normal incidence (Fig 2.3b). As the mean wave period increased and incident wave direction became more predominantly from the south, accretion began and was reinforced by low wave energy at the sea-land interface. The

onshore transport moved the ridge 1.5 m per day, while it accreted approximately 0.2 meters per day (Fig 2.9). From the first day of formation, 10/03, to the last day surveyed, 10/10, the ridge and runnel system accreted  $30 \text{ m}^2/\text{m}$  along the cross-shore transect at  $y = 600 \text{ m}$  (Fig 2.8c).

As waves run up the beach and over the ridge, there is no return flow back across the elevated ridge. Instead, the onshore directed water flows into the deep runnel (e.g., the lighter contours for  $90 < x < 100 \text{ m}$  and  $600 < y < 675 \text{ m}$  in Figs. 2.8b & 2.9a indicate that closer to the dune toe the bathymetry is lower than the ridge and the dune toe), and alongshore toward the north until it meets a cross-shore-oriented runoff channel and flows to the ocean. Remote sensing estimates of the flows in the runnel suggest current speeds as great as  $1 \text{ m/s}$  (personal communication from Alex Muscalus) that caused additional erosion and created mean-flow bedforms (not shown). Subsequent surveys to observe the destruction of the ridge and runnel were not obtained.

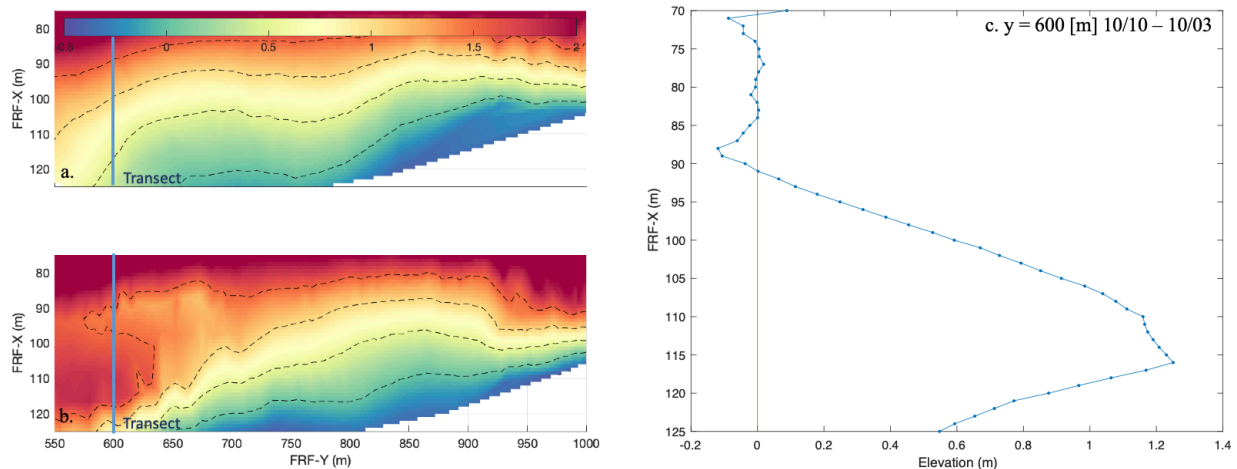


Figure 2.8: (a) Sand levels (color contours relative to NAVD88, key at top) measured with a backpack survey on 10/03 and (b) 10/10 2023 as a function of the cross-shore and alongshore coordinates. (c) Total change in sand levels along the transect for  $y=600$  (vertical lines) as a function of cross-shore coordinate during a ridge and runnel formation event.

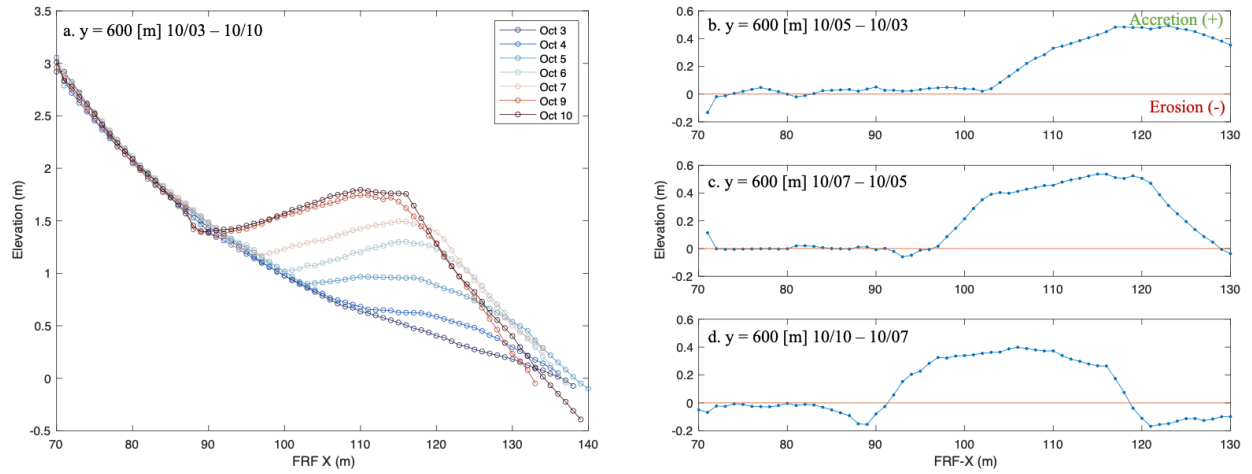


Figure 2.9: (a) Elevation along an alongshore transect ( $y = 600$  m) versus cross-shore coordinate between 10/03 and 10/10 (legend in the upper right), and daily elevation change versus cross-shore coordinate from (b) 10/03 to 10/05, (c) 10/05 to 10/07, and (d) 10/07 to 10/10.

## Chapter 3 Survey Technique Comparison

The time inefficiencies in conducting large area topographic surveys using a backpack global positioning receiver (GPS), as well as the practical limitation of having to be present at the location provide the opportunity for alternate technology to enhance the capabilities of analyzing the morphology of the coastline. This study investigated lidar systems as an alternative to backpack GPS systems. The lidar systems used here included a drone-based system for aerial surveys and a fixed-in-space (stationary) system with a lidar mounted on a pole above the dune. Drone based lidar (aerial) and stationary mounted lidar (terrestrial) were compared with each other and with the backpack surveys that were conducted daily and are considered ground truth. Utilizing lidar to survey the beach significantly minimizes the time required to conduct surveys, while maximizing spatial resolution using a high frequency pulse rate.

### 3.1 Backpack Surveys

Backpack surveys were conducted daily for three weeks and used as ground truth. The backpack survey equipment was comprised of a Trimble R7 GPS real time kinematic (RTK) modem receiver sampled at 10 Hz and housed in a hardened water-resistant casing attached to a strap and harness system to be worn on the back of a single surveyor. The modem is connected to a Trimble Zephyr Geodetic GPS antenna mounted on an aluminum pole that is welded into the backpack frame to extend above the surveyor to maintain a stable fixed height (Fig. 3.1). To provide accurate elevation and location, the backpack receiver collects GPS correction information from a tripod mounted Trimble Zephyr Geodetic GPS antenna at a verified GPS location on the northwest side at the beginning of the research pier at the FRF site. The data collected by the surveyor is corrected for elevation and position in post processing utilizing the base station receiver.





*Figure 3.1: Backpack apparatus with Trimble GPS receiver in yellow box on the left and the base station tripod and accompanying Trimble GPS antenna on the right.*

Backpack surveys were conducted daily, within an hour of low tide referenced to the NOAA tide charts. A single operator would activate the GPS base station at the tripod at the research pier and then the GPS housed in the backpack apparatus before going to the starting location of the survey area. All surveys were started in the southern region of the survey area along the research pier pilings at the toe of the dunes at  $x = 70$  and  $y = 550$  m. The survey pattern was selected to measure the slope of the beach with cross-shore transects separated by approximately 10 m for the entire 450 m length of the survey area (Fig. 2.1a). At the conclusion of the cross-shore transects, alongshore transects were completed at the same 10 m spacing as the cross-shore transects to resolve features with cross-shore structures, such as beach cusps. To maximize resolution of topographic features of interest (e.g., cusps, ridge and runnel), the operator would complete additional cross-shore and alongshore transects with 2-m spacing. Upon completion of the survey, the height was measured from the ground to the base of the GPS receiver at the top of the backpack apparatus for post processing error correction and to compensate for height



differences of multiple individuals that completed the surveys. The data from the backpack apparatus GPS receiver was post processed with the tripod base-station GPS receiver to provide corrected elevation relative to NAVD88. The entire surveying process for an area of this size required traversing 5-6 km of the beach daily, and took over an hour for each survey.

Backpack surveys were favored for ground truth based on the consistency at which they were conducted and the ability to maximize coverage from the dry beach into the inner surf zone. The backpack survey output was converted to local FRF coordinates and interpolated onto a 1- by 1- m grid along 50 m in the cross-shore and 450-m in the alongshore to create digital elevation models for day-to-day comparison and analysis of formation and destruction of topographic features (Fig 2.1b).

### **3.2 DJI Matrice 300 / Zenmuse L1 Lidar Payload**

The use of drone mounted lidar systems in topographic surveying provides an alternative to the backpack surveys, and reduces the personnel time investment. Lidar operates through a series of high pulse lasers on a repeating pattern that is capable of providing position and elevation at a high resolution. For this study, the DJI Matrice 300 with a Zenmuse L1 lidar payload (Fig. 3.2) was used to assess the applicability of the use of drone mounted lidar in coastal regions affected by the complexity of a dynamic surf zone.



*Figure 3.2: DJI Matrice M300 with Zenmuse L1 payload attachment.*

Drone mounted lidar systems maintain the ability to focus on a specific area of interest and personalize data collection priorities similar to the benefits of focused backpack surveys. Drone mounted systems also reduce the overall time required to survey a region relative to the time required for a backpack survey, providing the ability to conduct multiple surveys in succession within the same low tide cycle. Drone based lidar utilizes pre-planned flight paths for self-execution of missions from takeoff to flight completion, which further removes the human intervention and can be executed for data collection without personal knowledge of the survey priorities. For the area of interest in this study, the time required to survey the same 22,500 m<sup>2</sup> area with a drone lidar system was 15 minutes, less than the 1+ hr required for a backpack survey of the same area, and could be conducted multiple times within the hour buffer of low tide. Although the time required for each drone-based survey is reduced, the system employed in this study was restricted to wind speeds of less than 15 m/s (30 knots), which resulted in only nine

days of data collection during the three-week period of the study. Wind speeds regularly approached the maximum capabilities of the drone, and when wind speed did not inhibit flights, as windspeed increased, the time required to complete a full survey increased and battery life diminished such that multiple flights in the same low tide cycle were not possible.

The ability to modify the flight plan for the survey area of interest is a benefit of drone based lidar systems, contributing to the reduction of time required to conduct and obtain data, in contrast to daily backpack surveys. To compare the cross-shore and alongshore transects between the survey techniques used in this study, the flight pattern for the drone based lidar was designed to match the pattern designed for the backpack surveys (Fig 2.1c). The drone conducted a series of cross-shore transects starting at  $x = 70$  and  $y = 550$  m. All missions were conducted with consistent in-flight system settings flying at 60 meters altitude relative to pre-flight takeoff elevation, dual-pulse repetitive scanning pattern resulting in 480,000 pulses per second, and 80 percent overlap of each preceding transect line, all of which maximize resolution and ease of meshing the individual transect lines in post-processing. The Matrice 300 and Zenmuse L1 lidar payload communicate internally to the self-contained inertial navigation (INS) system to ensure the accuracy and stability of the system in three-dimensional space while in-flight, and utilizes the same benchmark GPS location and tripod-mounted Trimble Zephyr Geodetic antenna at the base of the FRF research pier to correct for elevation with respect to NAVD88 (38.876 m). The data output from the DJI post-processing software Terra was corrected a final time to account for the geoid consistent with the region that covers the Outer Banks, North Carolina. The corrected elevation data, converted to the local FRF coordinate system was interpolated on a 1- by 1-m grid fitted to the survey area for cross-shore and alongshore transect comparison to the backpack survey ground truth and the stationary lidar system employed at the north end of the survey area.

### **3.3 Stationary Terrestrial Lidar**

Stationary lidar systems provide an alternate method of remote topographical surveying. Stationary lidar systems have the same benefits as those of drone mounted lidar systems, but also have the ability to be run continuously without operator intervention, and reduce the constraints of environmental factors such as the wind. The disadvantage of these systems in contrast to

drone mounted systems is that the lidar must be mounted on-site and is not capable of surveying from a nadir vantage point to the area of interest, and thus is subject to errors caused by shadowing by features depending on the angle at which lidar pulses are projected and returned.

The continuously sampled stationary Riegl VZ-1000 terrestrial lidar system was mounted on the north end of the survey area above the dunes, and was sampled at 7 Hz. The scans covered the cross-shore distance to the waterline and 250 m in the alongshore (Coco et al. 2023). The lidar conducts a line scan survey every hour resulting in a 30-minute time series sweeping 237 degrees around the sensor (O’Dea, 2019). Output was converted to local FRF coordinates and interpolated onto a 1- by 1-m grid along 50 m in the cross-shore spanning the 250-m field of view in the alongshore. The dune lidar data sets were obtained from the CHL THREDDS Data Server (CHS TDS) (<https://chlthredds.erdc.dren.mil/thredds/catalog/frf/catalog.html>).

### **3.4 Survey Technique Comparison**

To compare and contrast the capabilities of the three systems employed during this study, the data sets were selected based on the days that a survey was conducted utilizing all three methods within an hour of low tide. The three data collection methods were evaluated using both alongshore and cross-shore transects extracted from the gridded data. The alongshore transect at  $x = 80$  m in the cross-shore on 10/02 was evaluated for the purpose of the inclusion of multiple complex topographic features in the field of view of each of the survey techniques (Fig 3.3). The transect was extended to the extent of the survey area that went beyond the distance limitations of the stationary terrestrial lidar that ends at  $y = 700$  m (Fig 3.3). In addition, two cross-shore transects were selected. The first was a smooth profile on 10/02 that was selected to compare the methods when all 3 systems were operating (Fig 3.4a), and the second transect (on 10/05) was selected to compare the drone mounted lidar with the backpack survey when there was a defined feature (the ridge and runnel, Fig 3.4b). The field of view of the stationary terrestrial lidar system did not extend to the entire survey area, and thus was not included in the cross-shore analysis of the ridge and runnel system. All three survey collection methods agree within 0.1 m in the vertical in the alongshore and the cross-shore.

The RMSE was evaluated between the backpack surveys and the drone lidar and the stationary lidar. Backpack surveys were used as ground truth in this study, and therefore were the basis for comparison when evaluating RMSE. Lidar to lidar systems were not evaluated. The RMSE between the backpack and drone lidar surveys were 0.04 m for the cross-shore transect (Fig 3.4a) with no noticeable features, 0.05 m when the ridge and runnel system was present, and 0.02 m for the alongshore transect (Fig 3.3) on Oct 02 when beach cusps were present. The RMSE between the backpack and dune lidar surveys were 0.04 m for the cross-shore transects (Fig 3.4a) and 0.05 m for the alongshore transect (Fig 3.3). The RMSE between the backpack and drone lidar surveys calculated over the 1- by 1-m spatial grid spanning the entire region ranged from RMSE = 0.05 to 0.09 m when the beach was relatively featureless to RMSE = 0.05 m when the beach cusp field and ridge and runnel systems were present.

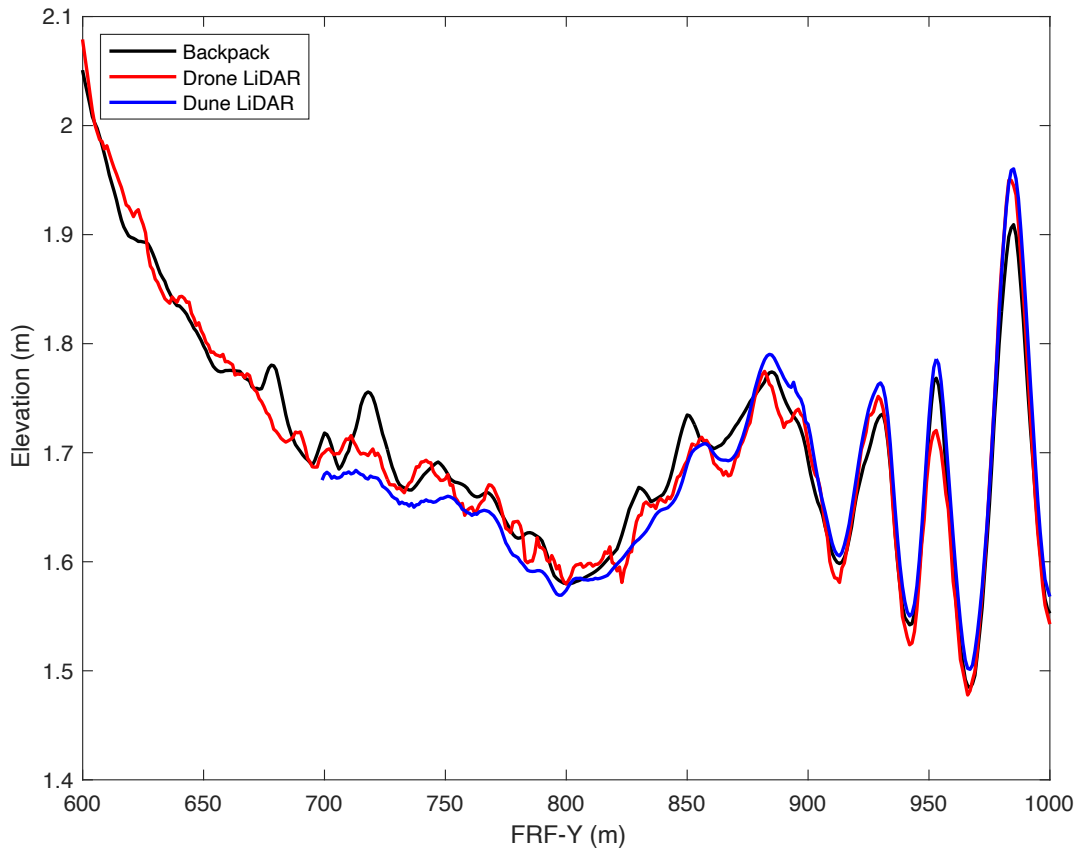


*Figure 3.3: Elevation of the beach versus alongshore coordinate for backpack (black), drone lidar (red), and stationary dune lidar (blue) surveys conducted on 10/02. Stationary dune lidar data (blue) adjusted 0.05 m to account for offset in raw data.*

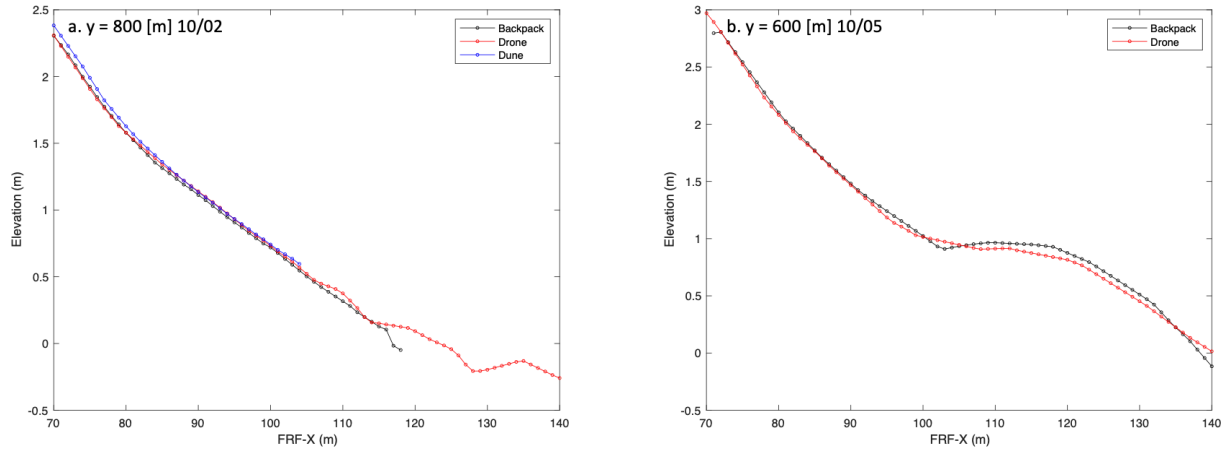


Figure 3.4: Elevation of the beach versus cross-shore coordinate for backpack (black), drone lidar (red), and stationary dune lidar (blue) surveys conducted on (a) 10/02 2023 and (b) 10/05 2023 (in b the dune lidar did not extend as far south as  $y=600$  m).

All survey techniques accurately represent the generated cusp field and varied morphology at a high resolution with a maximum difference in elevation between the survey techniques of 0.1 m between the drone lidar and the stationary lidar at the northern most cusp formation in the survey area at  $y = 1000$  m.

The dominant topographic feature in the northern region of the survey area between  $y = 700$  and  $y = 1000$  m was the formation and destruction of cusp fields. Based on the cross-shore orientation of cusp fields, cross-shore transects in the field of view of the stationary terrestrial lidar did not result in observable changing features in the cross-shore topography. The absence of complex features, resulted in smooth contours in the cross-shore transect of all three survey techniques with beach slope of 0.045 with a 2.25-m elevation change over 50 m from the toe of the dune to the water line at  $x = 115$  m, with an error of less than 0.05 m for the distance covered by all three survey techniques. The stationary terrestrial lidar field of view did not reach the waterline covering from the dune to  $x = 105$  m (Fig 3.4a, blue curve). At the water line, the drone lidar (Fig 3.4a, red) and the backpack survey (Fig 3.4a, black), begin to diverge. The backpack surveys were conducted to include survey coverage into the surf zone to knee deep water depth and the drone lidar provided survey coverage to  $x = 140$  m. A rapid drop in elevation at  $x = 115$  m as measured by the backpack survey was not registered by the drone lidar, indicating the inability to transition from topography to bathymetry accurately, which is a

significant limitation in coastal regions.

The ridge and runnel system was the dominant feature in the southern region of the survey area from  $y = 500$  to  $y = 700$  m. Based on the alongshore orientation of ridge and runnel systems, the elevated ridge and depressed runnel were observable by cross-shore transects. The field of view of the stationary terrestrial lidar did not extend to this region of the survey area and was therefore not included in the analysis. The slope of the beach from the dune to the runnel at  $x = 100$  m was 0.07, with a 2-m elevation change over 30 m, with no offset between the backpack survey and drone lidar (Fig 3.4b). The difference in survey techniques over the ridge to the water line at  $x = 135$  m was less than 0.05 m (Fig 3.4b). At the water line, the drone lidar (Fig 3.4b, red) and backpack survey (Fig 3.4b, black) diverge, consistent with prior observation of the inability of the drone lidar to provide accurate results when transitioning from dry beach topography to bathymetry in the surf zone.

## Chapter 4 Conclusions

The formation and destruction of a cusp field and the formation of a ridge and runnel over a three-week period on the beach at the Field Research Facility in Duck, North Carolina was observed with 3 surveys techniques. Three weeks of daily GPS equipped backpack surveys were performed at low tide to monitor the morphological evolution of the 22,500 m<sup>2</sup> of the coastline with respect to hydrodynamic forcing, and were used as ground truth for lidar surveys over the same area.

Both the cusp destruction and generation in the northern region of the survey area occurred over single tidal cycles, consistent with previous results. With respect to cusp destruction, the initial conditions observed were three prominent horns extending outwards toward the sea with two bays reinforcing the cusp system. Wave characteristics were favorable to sustaining the cusp system with low significant wave height and consistent incident wave direction. As the significant wave height increased, and the incident wave direction shifted, the cusp field was flattened and the planar beach face came to a steady state based on the new steady state wave conditions. Alternatively, the beach cusp formation process occurred during a period of sustained low energy waves. Initially a flat, planar beach face experienced a possible instability as the incident wave direction began to shift. Throughout the shift, the significant wave height remained low, which allowed for the reinforcement of the horn and bay systems by accreting sediment to the horns and eroding sediment through the bays until a steady state condition between sediment transport and wave conditions was reached, leaving a well-defined beach cusp system. The feedback processes between the sediment and hydrodynamic forcing resulted in a predominantly erosive process for cusp field destruction and an accretion process for cusp field formation that is reinforced and sustained by hydrodynamic forcing.

The formation of the ridge and runnel system occurred over a week, a longer timescale with respect to cusp field destruction and formation. The onshore migration of sediment occurred with low significant wave heights, but increasing wave period and shifting incident wave direction. The moderate wave conditions present throughout the formation and reinforcement were



consistent with previously observed onshore migration of ridge and runnel systems with a berm reinforced by accretion with an erosive channel on the land side of the ridge causing water to flow alongshore (north) before flowing offshore through an outflow channel. The ability to obtain data sets daily during ridge and runnel formation and onshore migration is important to analyze the volume and pace at which these systems evolve, which is a benefit of employing a survey system that is independent of sea state and meteorologic conditions in the survey area.

Remote sensing techniques such as lidar provide an alternative method to survey the beach. Two lidar systems were compared with the backpack surveys. A stationary lidar system mounted on a pole at one end of the survey site performed a topographic survey every hour, and a drone-mounted lidar flew over the area when weather conditions permitted. The elevations produced by the lidar systems were similar with those from the backpack surveys (considered ground truth), with RMS errors and biases both less than 0.1 m. Although the stationary lidar system provided hourly surveys 24 hrs/day, it was restricted in its field of view, and thus was capable of surveying only the north half of the area of interest. The drone mounted lidar covered the entire survey area, but was restricted by winds (resulting in data for 9 of the 21 days of backpack surveys). Drone systems are beneficial in that the time required to survey the area of interest of 22,500 m<sup>2</sup> was reduced from over 1 hr for a backpack survey to approximately 15 minutes. While the drone based lidar system increases the flexibility of defining survey areas based on its mobility, the system used in this study was not capable of penetrating the water column to observe the transition from topography to bathymetry, and thus resulted in inconsistent measurement in areas of significant wave runup.

## References

- Birkemeier, W. A. & Mason, C. (1984). "The CRAB: A Unique Nearshore Surveying Vehicle." American Society of Civil Engineers, *Journal of Surveying Engineering* 110(1): 1-7.
- Brodie, K. L., Conery, I., Cohn, N., Spore, N., & Palmsten, M. (2019). Spatial variability of coastal foredune evolution, part A: Timescales of months to years. *Journal of Marine Science and Engineering*, 7(5), 124. <https://doi.org/10.3390/jmse7050124>
- Coco, G., Burnet, T.K., Werner, B.T., Elgar, S. (2003). Test of self- organization in beach cusp formation. *J. Geophys. Res.*, 108(C3), 3101, 46.1–46.11.
- Coco, G., & Murray, A. B. (2007). Patterns in the sand: From forcing templates to self-organization. *Geomorphology*, 91(3–4), 271–290. <https://doi.org/10.1016/j.geomorph.2007.04.023>
- Cohn, N., Dickhudt, P., Brodie, K. (2022). Remote Observations of Aeolian Saltation, *Geophysical Research Letters*, 10.1029/2022GL100066, 49, 16
- Cohn, N., Brodie, K., Johnson, B., Palmsten, M. (2021). Hotspot dune erosion on an intermediate beach, 10.106/2021.103998, 170.
- DJI Zenmuse L1 Operation Guidebook, DJI, April 20, 2023. Accessed: April. 18, 2024. [Online]. [https://dl.djicdn.com/downloads/Zenmuse\\_L1/20230420/DJI\\_L1\\_Operation\\_Guidebook\\_V1.2.pdf](https://dl.djicdn.com/downloads/Zenmuse_L1/20230420/DJI_L1_Operation_Guidebook_V1.2.pdf)
- Forte, M. F., Birkemeier, W. A., Mitchell, J. R. (2017). Nearshore survey system evaluation, ERDC/CHL – TR-17-19.
- Guza, R. T., and R. E. Davis, Excitation of edge waves by eaves incident on a beach, *J. Geophys. Res.*, 79(9), 1285-1291, 1974.
- Luijendijk, A., Hagenaaars, G., Ranasinghe, R., et al. (2018). The State of the World's Beaches. *Sci Rep* 8, 6641 <https://doi.org/10.1038/s41598-018-24630-6>.
- Masselink, G., Kroon, A. (2002) Morphodynamics of intertidal bar morphology on a macrotidal beach under low-energy wave conditions, North Lincolnshire, England, 190, 591-608.
- Masselink, G., Kroon, A., and Davidson-Arnott, R. G. D. (2006). Morphodynamics of intertidal bars in wave-dominated coastal settings - a review, *Geomorphology*, 73, 33-49.
- Masselink, G. (2004). Formation and evolution of multiple intertidal bars on macrotidal beaches: application of a morphodynamic model, *Coastal Engineering*, 51, 713-730.

Mentaschi, L., Vousdoukas, M. I., Pekel, J.-F., Voukouvalas, E. & Feyen, L. (2018). Global long-term observations of coastal erosion and accretion. *Sci. Rep.* 8, 12876.

Michel, D., and Howa, H. L. (1999). Short-term morphodynamic response of a ridge and runnel system on a mesotidal sandy beach, *Journal of Coastal Research*, 15(2), 428-437.

O’Dea, A., Brodie K., Hartzell, P., Continuous Coastal Monitoring with an Automated Terrestrial Lidar Scanner, *Journal of Marine Science and Engineering*, 7, 37, (2019).

O’Dea, A., Brodie, K., Analysis of Beach Cusp Formation and Evolution Using High-Frequency 3D Lidar Scans, (2024). *Journal of Geophysical Research: Earth Surface*, 10.1029/2023JF007472, 129, 2.

Trimble R7/R8 GPS Receiver User Guide, Trimble (2003). Accessed: April. 18, 2024. [Online]. [https://www.ngs.noaa.gov/corbin/class\\_description/TrimbleR7-R8\\_UserGuide.pdf](https://www.ngs.noaa.gov/corbin/class_description/TrimbleR7-R8_UserGuide.pdf)

Vousdoukas, M.I., Ranasinghe, R., Mentaschi, L. et al. (2020). Sandy coastlines under threat of erosion. *Nat. Clim. Chang.* 10, 260–263, <https://doi.org/10.1038/s41558-020-0697-0>

Werner, B.T., Fink, T.M. (1993). Beach cusps as self-organized patterns. *Science* 260, 968–971.

Werner, B. T. (1999). Complexity in natural landform patterns, *Science*, 284, 102–104, 1999.